



Article

Prediction of Crops Cycle with Seasonal Forecasts to Support Decision-Making

Daniel Garcia ¹, Nicolas Silva ², João Rolim ¹, Antónia Ferreira ¹, João A. Santos ³, Maria do Rosário Cameira ¹ and Paula Paredes ¹,*

- LEAF—Linking Landscape, Environment, Agriculture and Food Research Center, Associate Laboratory TERRA, Instituto Superior de Agronomia, Universidade de Lisboa, Tapada da Ajuda, 1349-017 Lisboa, Portugal; dgarcia@isa.ulisboa.pt (D.G.); joaorolim@isa.ulisboa.pt (J.R.); aferreira@isa.ulisboa.pt (A.F.); roscameira@isa.ulisboa.pt (M.d.R.C.)
- ² Luiz de Queiroz College of Agriculture, University of São Paulo, Piracicaba 13418-900, Brazil; nicolascruz.usp@usp.br
- CITAB—Centre for the Research and Technology of Agro-Environmental and Biological Sciences, Inov4Agro—Institute for Innovation, Capacity Building, and Sustainability of Agri-Food Production, University of Trás-os-Montes e Alto Douro, UTAD, 5000-801 Vila Real, Portugal; jsantos@utad.pt
- * Correspondence: pparedes@isa.ulisboa.pt

Abstract: Climate variability, intensified by climate change, poses significant challenges to agriculture, affecting crop development and productivity. Integrating seasonal weather forecasts (SWF) into crop growth modelling tools is therefore essential for improving agricultural decision-making. This study assessed the uncertainties of raw (non-bias-corrected) temperature forecasts from the European Centre for Medium-Range Weather Forecasts (ECMWF) SEAS5 seasonal (seven-month forecasts) to estimate the spring-summer maize, melon, sunflower, and tomato crops cycle from 2013 to 2022 in the Caia Irrigation Scheme, southern Portugal. AgERA5 reanalysis data, after simple bias correction using local weather station data, was used as a reference. The growing degree-day (GDD) approach was applied to estimate the crop cycle duration, which was then validated against ground truth and satellite data. The results show that SWF tend to underestimate maximum temperatures and overestimate minimum temperatures, with these biases partially offsetting to improve mean temperature accuracy. Forecast skill decreased non-linearly with lead time, especially after the second month; however, in some cases, longer lead times outperformed earlier ones. Temperature forecast biases affected GDD-based crop cycle estimates, resulting in a slight underestimation of all crop cycle durations by around a week. Nevertheless, the forecasts captured the overall increasing temperature trend, interannual variability, and anomaly signals, but with marginal added value over climatological data. This study highlights the potential of integrating ground truth and Earth observation data, together with reanalysis data and SWF, into GDD tools to support agricultural decision-making, aiming at enhancing yield and resources management.

Keywords: temperature; growing degree-days; ERA5 reanalysis data; decision-support

check for **updates**

Academic Editor: Gniewko Niedbała

Received: 12 April 2025 Revised: 20 May 2025 Accepted: 20 May 2025 Published: 24 May 2025

Citation: Garcia, D.; Silva, N.; Rolim, J.; Ferreira, A.; Santos, J.A.; Cameira, M.d.R.; Paredes, P. Prediction of Crops Cycle with Seasonal Forecasts to Support Decision-Making. *Agronomy* **2025**, *15*, 1291. https://doi.org/10.3390/agronomy15061291

Copyright: © 2025 by the authors. Licensee MDPI, Basel, Switzerland. This article is an open access article distributed under the terms and conditions of the Creative Commons Attribution (CC BY) license (https://creativecommons.org/licenses/by/4.0/).

1. Introduction

Climate variability represents a major source of uncertainty in agriculture and has been exacerbated by climate change. This impacts crop development and productivity [1–5]. The Mediterranean region, a climate change hotspot [6,7], is experiencing raising temperatures, shifting precipitation patterns, and an increase in extreme weather events, such as droughts and heatwaves (e.g., [8]). Such events can disrupt crop growth conditions and ultimately

threaten agricultural production [9–11]. Climate variability further increases the complexity of agricultural production and the decision-making processes of farmers and other stakeholders. Uncertainty about future weather conditions hampers seasonal planning, increases risks, and frequently results in production and economic losses. It may also have negative environmental impacts [12–14]. Therefore, accessible and innovative tools are needed to support decision-making and to help cope with climate uncertainty [15]. This could be achieved through the use of early warning systems and the integration of climate forecasts into crop growth modelling tools and resource management strategies [16–19].

Crop growth and productivity are highly dependent on climatic conditions, particularly temperature [20–23]. Changes in the temperature regimes affect the crop development rates, ultimately impacting quantity and quality of yields [24,25]. Several authors have reported that, in the absence of major biotic and abiotic stresses, crop development rates are generally assumed to be linearly related to temperature. This relationship is used in the growing degree-days (GDD) approach [21,26,27]. The GDD approach accumulates heat units above a lower threshold temperature (base temperature) and considers an upper limit above which development stops. This provides a simplified yet effective way of estimating crop growth stages and crop cycle duration. Although more complex modelling approaches are widely used, particularly to simulate crop—climate interactions, e.g., AquaCrop crop growth model [28], they require extensive input data, calibration, and technical knowledge, making them less accessible for routine use by farmers, water managers or technicians [29]. In contrast, the GDD approach provides a practical and intuitive decision-support tool that enables timely adjustments in agricultural planning and management. Therefore, GDD-based estimates are particularly suitable for operational applications [30,31].

Seasonal forecasts (SWF) aim to provide insight into the expected weather conditions over the coming months, as well as any deviations from long-term averages. Despite the inherent unpredictability of the atmosphere, advances in modelling have improved the reliability of these forecasts, establishing them as valuable decision-making tools in agriculture [32–34]. Several studies have focused on using SWF to estimate the timing of specific phenological stages [35,36], as well as for predicting early season yields [18,37–42]. Furthermore, some studies have emphasised the added value of using SWF compared to historical climatological data in an agricultural context [43–45]. Although SWF have limitations, such as varying accuracy depending on region, season and variables of interest [35,46,47], recent studies show that integrating seasonal temperature forecasts with crop growth models can effectively support decision-making by providing early estimates of crop development and productivity [16,48,49]. However, their practical application in Mediterranean agriculture remains limited due to uncertainties in forecast accuracy and the complexity of their use [50,51].

Incorporating seasonal temperature forecasts into a GDD tool enables proactive adjustments to planting and harvesting. This helps farmers adapt to climate variability and mitigate the risks associated with unpredictable seasonal shifts (e.g., early frosts, heatwaves or droughts). It will also enable more efficient resources management, particularly water, and promote yield optimisation by ensuring that crops develop within specific time windows. This study aims to assess how accurately the raw (non-bias-corrected) seasonal temperature forecasts, provided by the European Centre for Medium-Range Weather Forecasts (ECMWF) SEAS5 predict the duration of spring–summer crop cycles in a water-scarce region of southern Portugal. The specific objectives of this work are: (1) to assess the accuracy and skill of the SWF in predicting maximum, minimum, and mean temperature; (2) to evaluate the influence of lead time on forecast performance; (3) to estimate the performance of crop cycle length estimation using the GDD approach driven by SWF. The novelty of the current study lies in the comprehensive assessment of the practical utility of seasonal

forecasts for supporting agricultural decision-making, achieved by combining direct validation of temperature forecast skill and indirect validation of its accuracy in estimating crop growth cycles. This study is a step towards identifying the practical potential and constraints to the widespread adoption of such simplified tools.

2. Materials and Methods

This study analyses the quality, skill, and usability of SWF data produced by the ECMWF for predicting the duration of the growing cycle of various spring–summer crops. This assessment used the SWF temperature data ingested in the GDD approach. The procedure followed the flowchart in Figure 1 and included the collection and Quality Assurance and Quality Control (QAQC) assessment of the different sources of temperature, i.e., the observed weather data (2013–2022), the AgERA5 reanalysis data, and SWF data. Ground truth and remotely sensed crop cycle data from previous studies [52] developed in the targeted Caia Irrigation Scheme were used as a baseline for the GDD approach. The need for bias correction of the AgERA5 reanalysis data were assessed prior to its use. After appropriate bias correction, the AgERA5 data were used as "observations" in the direct validation of the SWF data. The indirect validation of the SWF was performed by analysing the estimated crop cycle lengths using the cumulative GDD approach (Figure 1).

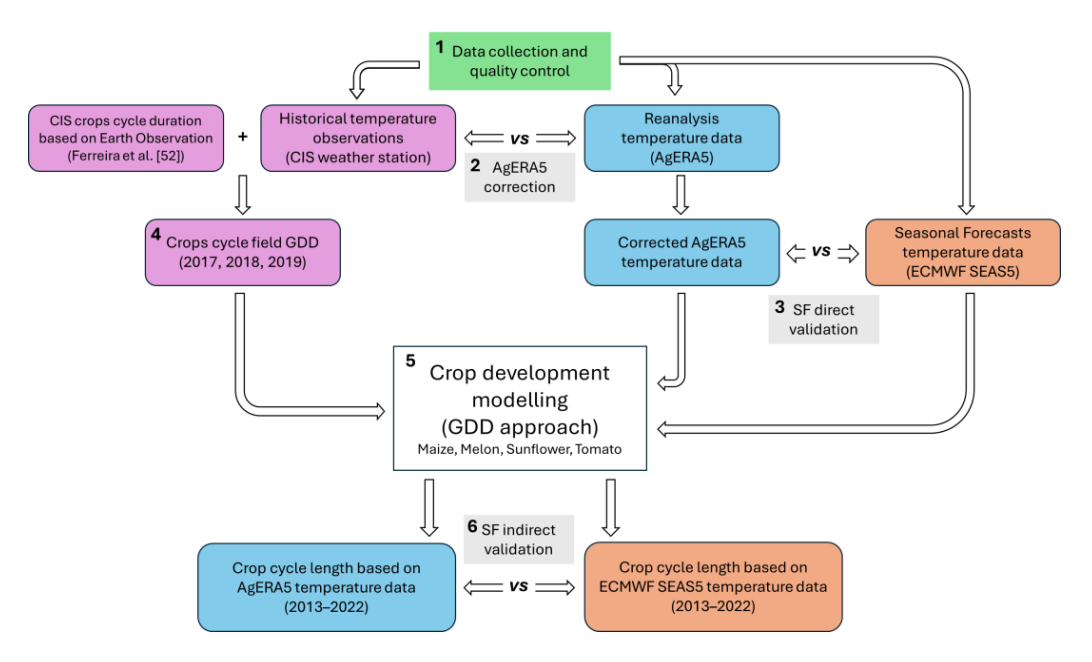


Figure 1. Flowchart with the schematic representation of the seasonal forecast assessment procedure. CIS—Caia Irrigation Scheme; GDD—Growing Degree-Day; SF—Seasonal Weather Forecasts.

2.1. Study Site Brief Characterisation

The current study was conducted at the Caia Irrigation Scheme (CIS) in Elvas, Alentejo region, southern Portugal (Figure 2). The CIS has been in operation since 1969 and is currently managed by the Caia Water Users Association (Caia WUA). It covers an area of approximately 7000 hectares and supplies water to over 800 farmers [52]. Water from the Caia Reservoir on the Caia River is distributed through an open channel system with upstream control, following a fixed rotation schedule that limits water allocation per hectare to each farmer. Irrigation is mainly drip irrigation (82%), followed by sprinkler irrigation (17%)—mainly center pivots—while surface irrigation accounts for approximately 2% of the total irrigated area.

Agronomy 2025, 15, 1291 4 of 23

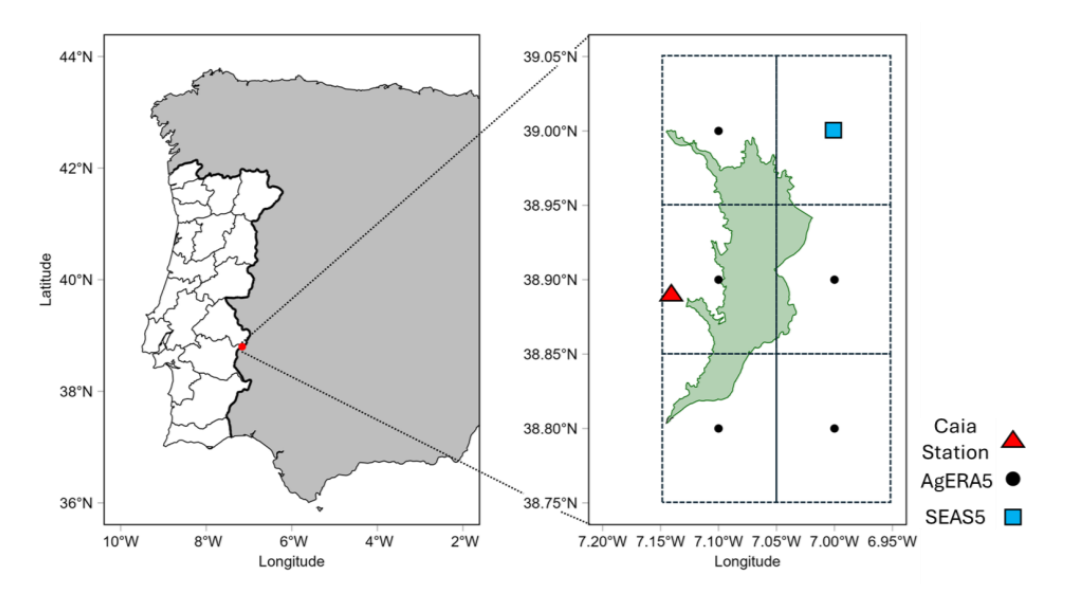


Figure 2. Localization of the Caia Irrigation Scheme, Elvas, Portugal, weather station, reanalysis, and SWF grids.

According to the Caia WUA, cropping patterns in the CIS have changed in recent decades, shifting from annual crops to highly profitable permanent orchards, primarily of olive (*Olea europaea* L.) and nuts (almonds and walnuts). Currently, olive orchards are the main crop in the CIS [52,53]. However, annual crops such as maize, winter cereals, processing tomato, and various oilseed and vegetable crops remain an important part of CIS production. For the current study, the main irrigated crops were selected, i.e., maize (*Zea mays* L.), melon (*Cucumis melo* L.), sunflower (*Helianthus annuus* L.) and tomato (*Solanum lycopersicum* L.).

According to the FAO classification [54], the main soils in the CIS are Fluvissols (45%), Luvissols (30%), and Calcissols (19%). Overall, the soils in the CIS are well-suited for irrigated agriculture, with a variety of textures (loamy-sand, silty-clay, clay) and structure, adequate drainage capacity, and gentle slopes (<6%) [55].

The region has a typical temperate Mediterranean climate, characterised by hot and dry summers. According to the Köppen–Geiger classification [56], it is classified as a Csa. The long-term (2002–2021) average annual precipitation is approximately 505 mm, of which around 25% occurs between April and September. The mean temperature is around 16.7 $^{\circ}$ C. The average maximum temperature exceeds 30 $^{\circ}$ C during the summer months, while the average minimum temperature falls below 5 $^{\circ}$ C in the winter months (Figure 3). The Elvas region is considered a climate change hotspot, so preparedness and adaptation measures are essential [57,58].

2.2. Atmospheric Data

2.2.1. Ground Truth Data

The ground-based meteorological data were obtained from a weather station belonging to the operational network of automatic agrometeorological stations installed across the major irrigated areas of the Alentejo region. This network is managed by the Centro Operativo e de Tecnologia de Regadio (COTR). The station is located within a 5×5 m grass-covered area, and comprises a central data acquisition unit, and a set of sensors. Air temperature is measured using a Thies Clima thermohygrometer (model 1.1005.54.000), with a measurement range of -30 to $70\,^{\circ}\text{C}$ and a response time of 20 s. Sensor readings are taken every 10 s and compiled into hourly and daily reports. The data are stored in Data Taker 500 loggers and transmitted automatically between 01:00 and 02:00 each day.

Agronomy **2025**, 15, 1291 5 of 23

Daily validated data are made available to users through the COTR platform. Further information is provided by Oliveira et al. [59]. Daily maximum (T_{max} , °C) and minimum (T_{min} , °C) temperature weather data covering the period 2013–2022 was collected from the meteorological station of Caia, Elvas (38°53′27″ N, 07°08′23″ W, 208 m a.s.l) which is located close to the CIS and within a 10 km radius of the crop plots observed during 2017–2019.

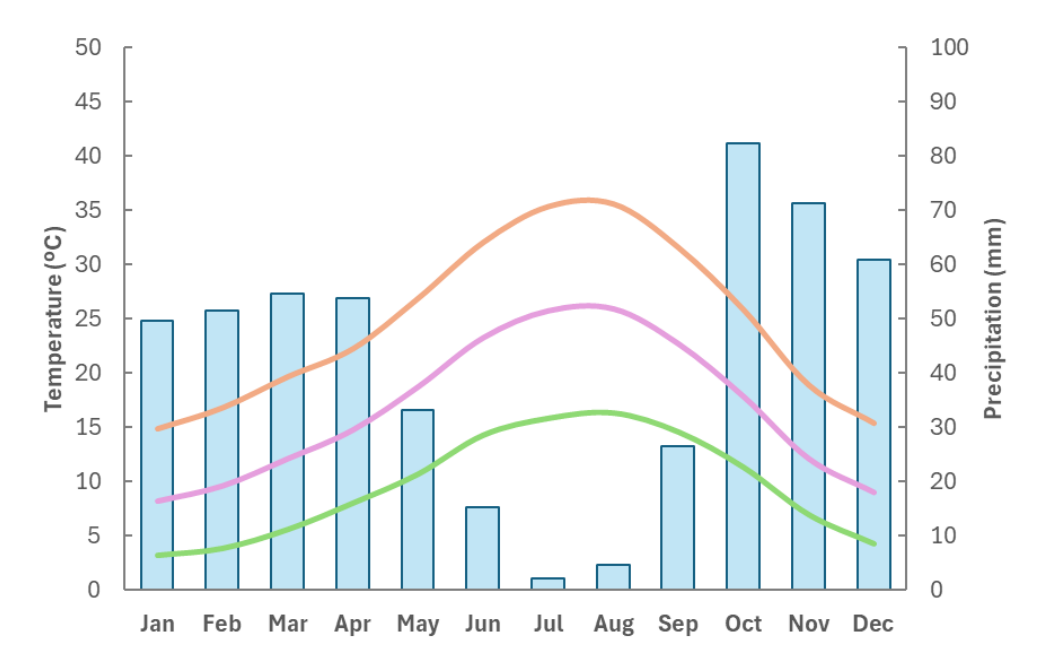


Figure 3. Long-term (2002–2021) historical meteorological characterisation of the Caia Irrigation Scheme (38 $^{\circ}53'27''$ N, 07 $^{\circ}08'23''$ W, 208 m a.s.l.), Elvas, Portugal. (Blue bars—precipitation; orange line— T_{max} ; pink line— T_{mean} ; green line— T_{min}).

2.2.2. Reanalysis

To address the issue of the point location weather dataset and, therefore, upscaling to the CIS, a reanalysis dataset was considered for this study. The AgERA5 (version 1.1) daily reanalysis dataset provided by the ECMWF and available in the Copernicus Climate Change Service Data Store was selected [60]. The AgERA5 dataset is based on the forcing of ECMWF ERA5 hourly data and has been developed for agricultural and agroecological studies (e.g., [61,62]). AgERA5 covers the period from 1979 to the present day, (one month prior to the date of access) on a global grid with a resolution of 0.1° and includes a large number of atmospheric and surface variables. In the current study, the six grid cells covering the CIS area were selected, and $T_{\rm max}$ and $T_{\rm min}$ data for the decade 2013–2022 were collected. To account for the differences in altitude between the weather station and the reanalysis grid points, a temperature correction was applied using a constant lapse rate, i.e., ratio of the variation in temperature and the variation in altitude, of 6.5 °C per km. This is a standard value for mid-latitude regions [63–65]. This adjustment improved the agreement between the reanalysis and the observed temperatures.

2.2.3. Seasonal Forecasts

The seasonal forecast data were provided by the European Centre for Medium-Range Weather Forecasts (ECMWF). This dataset is part of the Copernicus Climate Change Service (C3S) multi-system seasonal forecast service and is available from the Copernicus Climate Data Store (CDS) as "Seasonal forecast daily and sub-daily data on single levels". It is produced by the ECMWF SEAS5 (v5.1) system [66]. The dataset consists of an ensemble of gridded data with global coverage and a horizontal resolution of 1°, with temporal

Agronomy **2025**, 15, 1291 6 of 23

coverage from 1981 to the present day (with a one-month lag). The dataset includes hindcasts (1981 to 2016) with 25 ensemble members and real-time forecasts (2017 to the present day) with 51 ensemble members, extending 7 months into the future [32]. Daily T_{max} and T_{min} forecasts, initialised on 1 April for mainland Portugal, were collected to cover the spring–summer season; thus, the crop cycle of all the selected crops (Table 1). The analysis below focuses on the period 2013 to 2022, using data from the grid cell closest to the CIS (39°00′00″ N, 07°00′00″ W, 294 m a.s.l.). The CIS is entirely contained within a single SEAS5 grid cell and the grid point closest to it was selected as representative of the region. As each SEAS5 grid point represents an average condition within its cell, the selected point is considered to adequately capture the average conditions within the study area.

Year	Sowing/ Planting	Harvest	Length	CGDD		
2017	Apr 25	Sep 8	137	1929		
2018	May 7	Sep 11	128	1668		
2019	Apr 12	Sep 8	150	1827		
2017	Apr 30	Aug 29	122	1753		
2018	Not available					
2019	May 7	Aug 21	107	1366		
2017	May 20	Sep 23	127	2155		
2018	Apr 27	Aug 22	118	1619		
2019	Apr 12	Aug 11	122	1619		
2017	Apr 25	Sep 1	130	2173		
2018	-	Not av	ailable			
2019	Apr 2	Aug 11	132	1784		
	2017 2018 2019 2017 2018 2019 2017 2018 2019 2017 2018	Planting 2017	Year Planting Harvest 2017 Apr 25 Sep 8 2018 May 7 Sep 11 2019 Apr 12 Sep 8 2017 Apr 30 Aug 29 2018 Not av 2019 May 7 Aug 21 2017 May 20 Sep 23 2018 Apr 27 Aug 22 2019 Apr 12 Aug 11 2017 Apr 25 Sep 1 2018 Not av	Year Planting Harvest Length 2017 Apr 25 Sep 8 137 2018 May 7 Sep 11 128 2019 Apr 12 Sep 8 150 2017 Apr 30 Aug 29 122 2018 Not available 2019 May 7 Aug 21 107 2017 May 20 Sep 23 127 2018 Apr 27 Aug 22 118 2019 Apr 12 Aug 11 122 2017 Apr 25 Sep 1 130 Not available		

Table 1. Crop cycle characteristics derived from NDVI satellite data (2017–2019).

2.3. Data Analysis

2.3.1. Quality Assurance and Quality Control (QAQC)

The integrity and quality of weather data, whether from weather stations or gridded datasets, must be assessed prior to use. Poor sensor calibration, malfunctions, or limited maintenance can affect weather station measurements for different variables [67,68]. Conversely, modelled data often exhibits some bias [63,69–72]. Therefore, analysing data consistency is mandatory, and data corrections should be applied if necessary to address these issues [73]. The temperature data collected for this study underwent a QAQC process, during which missing, duplicate, and suspicious records were identified and corrected as necessary. The range and seasonal pattern of temperature values were examined to ensure that no records showed maximum temperatures lower than minimum temperatures. The T_{max} and T_{min} values were then used to calculate the daily mean temperature (T_{mean}) for the three datasets.

2.3.2. Reanalysis Data Bias Correction and Validation

A set of goodness of fit indicators was used to compare T_{OBS} and T_{REAN} in order to assess the need for bias correction, including the following: (i) the regression coefficient (b₀) of a forced to the origin (FTO) linear regression; (ii) the coefficient of determination (R^2) of an ordinary least squares (OLS) linear regression; (iii) the root mean square error (RMSE); (iv) the normalised root mean square error (NRMSE, %), calculated as the ratio of the RMSE to the mean of the observed values (\overline{O}), providing a dimensionless measure of the relative error of the model; and (v) the Nash and Sutcliff [74] model efficiency (EF). A similar approach has been used in previous studies [63,71,75–77].

Agronomy 2025, 15, 1291 7 of 23

The use of these metrics highlighted the need for bias correction in the reanalysis data. A simplified approach was adopted for both T_{max} and T_{min} by adding a constant c(month) to the uncorrected $T_{REAN\ unc}$ as follows:

$$c(month_i) = \overline{T_{REAN\ unc}(month_i)} - \overline{T_{OBS}(month_i)}$$
 (1)

Due to the small temperature differences within the study area, the correction factor for each variable was calculated using the reanalysis grid point closest to the Caia weather station $(38^{\circ}53'60''\ N,\,07^{\circ}05'60''\ W,\,226\ m\ a.s.l.)$ and then applied to all reanalysis grid points within the CIS.

2.3.3. Seasonal Forecasts Direct Validation Approach

The first assessment of SWF performance was based on a direct comparison between temperature data from the reanalysis dataset and SWF datasets for the same period (2013–2022). Temperature values were assessed at two levels, monthly and seasonal. The monthly assessment evaluated whether the SWF performance remained consistent over time (April, May, June, July, August, September, October). The seasonal analysis evaluated the overall forecast performance by averaging both $T_{\rm max}$ and $T_{\rm min}$ during April–September. This type of analysis uses a combination of the deterministic approach, which uses the SWF ensemble median, and a probabilistic approach, which uses all members of the forecast ensemble. The methodology adopted for each indicator is summarised in Table A1. The average of the six AgERA5 grid points was used as the reference for the comparison.

Analytical and statistical approaches were used to evaluate the precision and reliability of the ECMWF SEAS5 seasonal forecasts for the CIS. The analytical analysis involved producing box and whisker plots showing the forecast ensemble members along-side the reanalysis values for seasonal averages of T_{max} , T_{min} and T_{mean} . This approach made it possible to visualise errors in the SWF in relation to reanalysis, and to assess the ability of the forecasts to detect temperature anomalies and trends. In addition to the above mentioned goodness of fit indicators, other statistical performance metrics were used to quantify the accuracy and skill of the SWF for each variable (T_{max} , T_{min} and T_{mean}): Bias Percentage (PBIAS), Mean Absolute Error (MAE), Standardised Anomaly Index (SAI) [78,79], Anomaly Correlation Coefficient (ACC) [80] and Continuous Ranked Probability Skill Score (CRPSS) [80–84]. Table A1 summarises the information relative to each indicator.

Significance tests were conducted to evaluate the statistical significance of forecast performance metrics. Pearson's correlation t-test was used for ACC indicator to assess whether the correlation between reanalysis and forecasted anomalies differed from zero, while one-sample t-tests were applied for MAE and PBIAS to determine whether the mean absolute differences and mean differences (bias), respectively, were significantly different from zero ($\alpha = 0.05$).

2.3.4. Seasonal Forecasts Indirect Validation Approach

In this study, the performance of SWF was evaluated using an indirect approach by analysing its performance in calculating crop growth stages and cycle length. The time required for a plant to reach a given growth stage is directly related to the amount of temperature accumulation over time [21,85,86]. This relationship is referred to as growing degree-days (GDD). Therefore, the GDD approach was used to determine the length of the crop cycle. In the current study, it was assumed that GDD represents the cumulative sum of temperatures above a baseline threshold (T_{base}) required to reach a given growth

Agronomy 2025, 15, 1291 8 of 23

stage [20], and that development ceases above an upper temperature limit (T_{upper}) [27,86]. Therefore, GDD values were computed as follows:

$$GDD = \begin{cases} 0, & T_{mean} \leq T_{base} \\ T_{mean} - T_{base}, & T_{base} < T_{mean} < T_{upper} \\ T_{upper} - T_{base}, & T_{mean} \geq T_{upper} \end{cases}$$
 (2)

The crop cycles for the crops selected for the current study were derived from a thorough analysis of vegetation indices (NDVI) using Google Engine tools (Table 1). This analysis was conducted for the 2017, 2018, and 2019 years across the main production areas of maize, melon, sunflower, and tomato crops within the CIS. These durations represent the mean values of crop cycle durations across all farms within the CIS that cultivated each selected crop. In other words, they are the mean values of the ensemble of farms. The durations were validated using ground truth data provided by the Caia WUA, and some farms were surveyed in 2017. Melon and tomato crops were not identified within the study area in 2018. Further details on image processing can be found in the study by Ferreira et al. [52].

Having determined the length of each growth stage in days, the cumulative growing degree-days (CGDD) requirements were calculated using the observed (weather station) temperature data (Table 1). These CGDD values are within the reference values proposed by Pereira et al. [68] for crops not subject to biotic and abiotic stresses and were applied throughout the study period to determine crop cycles using reanalysis and SWF data.

Two types of analysis were performed. The first was a decadal analysis (2013–2022) that used 2017 GDD data as a reference (Table 2). This reference was maintained in the other years to evaluate the impact of climate variability on the forecast performance for crop cycle prediction. According to the Caia WUA, the sowing/planting and harvesting dates in 2017 are closer to the usual dates in the CIS. Therefore, the results presented in this study refer to 2017. The second analysis focused on the three years with NDVI-derived phenology data and considered CGDD variability across 2017, 2018, and 2019.

Table 2. Temperature and CGDD requirements to complete each crop growth stage and for the total crop season for maize, melon, sunflower, and tomato in Caia Irrigation Scheme, Portugal (Adapted from Ferreira et al. [52]).

Crop	Sowing/ Planting	Length (Days)	T _{base} (°C)	T _{upper} (°C)	Initial CGDD _{ini}	Develop. CGDD _{dev}	Mid-Season CGDD _{mid}	Harvest CGDD _{late}	Total CGDD
Maize	25 Apr	137	10	32	136	342	856	596	1929
Melon	30 Apr	122	10	38	356	428	525	445	1753
Sunflower	20 May	127	8	30	392	574	738	451	2155
Tomato	25 Apr	130	7	28	347	646	944	236	2173

 T_{base} is the base temperature (°C); T_{upper} is the cut-off temperature (°C); CGDD is the cumulative growing degree-day; Develop.—development stage.

The same statistical metrics used in the direct validation were applied to the crop cycle lengths (Table A1) to assess the performance of ECMWF SEAS5 forecasts in accurately predicting the crop cycle length, thus supporting crop management decisions in southern Portugal.

3. Results and Discussion

3.1. Reanalysis Correction and Validation

The analysis showed that the T_{max} and T_{min} reanalysis data are highly correlated with the weather station observations, with R^2 values above 0.98. However, the reanalysis data show a general tendency to underestimate T_{max} (b_0 = 0.94) and to overestimate T_{min} (b_0 = 1.15) compared to the observations (Figure 4). Table 3 summarises the accuracy of the reanalysis estimates relative to the observations before and after the simplified bias correction. The results show small errors for T_{max} (NRMSE < 10%), while the errors for T_{min} are quite high (NRMSE = 26%). The EF values for both T_{max} and T_{min} are high (>0.80). As T_{max} and T_{min} have opposite tendencies, the T_{mean} results are much better, with NRMSE < 6% and EF = 0.98. After the simplified bias correction, based on monthly mean differences between the observed and reanalysis data, the performance of the reanalysis temperature estimates for T_{max} , T_{min} , and T_{mean} improves. Initial biases and estimation errors are substantially reduced, particularly for T_{min} , with the NRMSE decreasing to 16%. This confirms the validity and appropriateness of the correction approach. The good results obtained for T_{mean} are further improved after bias correction. This leads to consistent and accurate agreement between the reanalysis and the observed data.

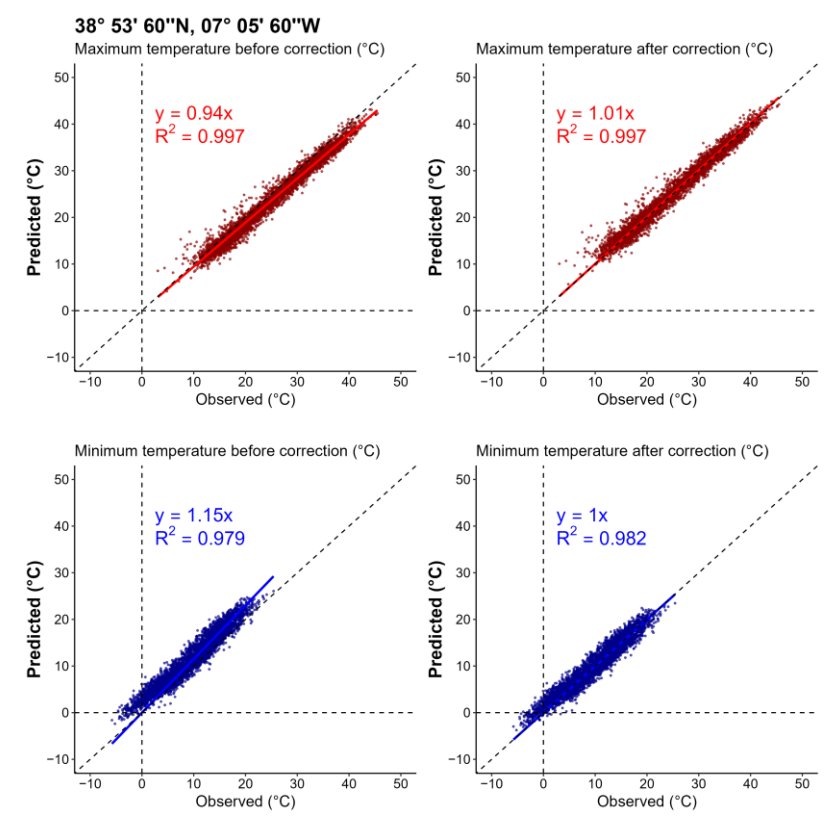


Figure 4. Comparison of ground truth (observed) and reanalysis (predicted) maximum (•) and minimum (•) temperature data (**left**) before correction and (**right**) after correction.

The results of this study are consistent with those reported in the literature, which highlight the good performance of various reanalysis products in reproducing temperature variables, particularly ERA5, for which R^2 values are generally above 0.90. Several studies have reported RMSE values around 2 °C when comparing reanalysis data with ground truth data. Examples include the study by Vanella et al. [76], which was carried out at several locations in Italy, including island environments, and the study by Jiménez-Jiménez et al. [87] which was carried out in Mexico. In line with our results, other authors (e.g., [87,88]) have found that reanalysis T_{mean} generally performs better than T_{max} and

 T_{min} , while a better agreement is often found for T_{max} than for T_{min} [63,75,89]. Several studies have reported that reanalysis datasets tend to slightly underestimate T_{max} and overestimate T_{min} before bias correction, including studies in Italy [75,77,89], Greece [90], and Portugal [63], as well as studies on a global scale [88]. Simple bias corrections based on monthly regional mean differences between ground-based measurements and reanalysis data may be an effective tool to improve the performance of reanalysis data [89].

Table 3. Statistical comparison between observed maximum, minimum, and mean temperature and the AgERA5 reanalysis (±standard deviation) (2013–2022).

	Maximum 7	Temperature	Minimum 7	Temperature	Mean Temperature	
Indicators	Before Bias Correction	After Bias Correction	Before Bias Correction	After Bias Correction	Before Bias Correction	After Bias Correction
b_0	0.94 ± 0.01	1.01 ± 0.01	1.15 ± 0.02	1.00 ± 0.02	1.02 ± 0.01	1.01 ± 0.00
RMSE ($^{\circ}$ C)	1.89 ± 0.08	1.21 ± 0.40	2.52 ± 0.25	1.57 ± 0.12	1.02 ± 0.04	0.98 ± 0.03
NRMSE (%)	7.62 ± 0.32	5.58 ± 0.17	25.88 ± 2.52	16.13 ± 1.18	5.88 ± 0.21	5.63 ± 0.19
EF	0.95 ± 0.01	0.97 ± 0.00	0.80 ± 0.04	0.92 ± 0.01	0.98 ± 0.00	0.98 ± 0.00

 b_0 is the regression coefficient; RMSE is the root mean square error; NRMSE is the normalised RMSE; EF—Nash and Sutcliff [74] model efficiency.

In summary, the reduction in RMSE and NRMSE values, together with the increase in the EF values, demonstrates that the applied correction effectively reduced systematic errors and improved agreement with the observed data.

3.2. Seasonal Forecasts Direct Validation

Direct validation involves comparing the ECMWF SEAS5 seasonal temperature forecasts with the AgERA5 gridded data. This allowed the assessment of the forecast system's performance in predicting temperature at both seasonal and monthly scales over the CIS.

3.2.1. Monthly Validation

As SWF covers a long period of time (seven months), it is important to assess their usefulness not only in terms of overall seasonal performance, but also at different stages within this period. The statistical accuracy indicators do not show a clear tendency for forecast performance to deteriorate with increasing lead time (Table 4). Errors do not consistently increase (or decrease) with the lead time; therefore, the seventh month is not necessarily the worst across all variables, nor is the performance of the first month necessarily the best (although it tends to be the more accurate for $T_{\rm min}$ and $T_{\rm mean}$). It should be noted that the MAE is significantly different from zero for all variables in all months. However, in the case of PBIAS, although there is a significant bias in all months for $T_{\rm min}$, the same is not true for $T_{\rm mean}$, for which there is only a significant bias in the fourth and fifth months (Table 4).

The results also show high dispersion of the SWF-reanalysis temperature pair, particularly after the first lead month. Therefore, the results suggest that forecast accuracy may be influenced not only by the temporal distance from the initialization date of the forecast, but also by other factors, such as the intrinsic climatic characteristics of each target month [91–93]. For example, depending on the target variable, regional climate dynamics and variability patterns, mid-summer months such as July and August may be more predictable than transition months such as April. This is true for T_{max} but not for T_{min} . These results are in line with previous studies. For instance, Lalic et al. [38] reported that temperature forecasts for May and June have a lower RMSE than those for March and April. Similarly, Santos et al. [41] reported lower MAE in summer months compared to transition months such as April or September, despite the forecast lead time.

Variable	Statistical Indicator	1st Month (April)	2nd Month (May)	3rd Month (June)	4th Month (July)	5th Month (August)	6th Month (September)	7th Month (October)
	PBIAS (%)	8.54 *	9.20 *	1.49	-0.03	1.09	2.11	10.27 *
	MAE (°C)	1.91 *	2.73 *	1.53 *	1.68 *	1.15 *	1.70 *	2.70 *
	RMSE (°C)	2.16	3.04	1.94	1.93	1.34	1.86	3.24
T_{max}	NRMSE (%)	9.78	11.10	6.16	5.39	3.74	5.91	12.29
	\mathbb{R}^2	0.52	0.48	0.00	0.30	0.09	0.06	0.07
	ACC	0.72 *	0.69 *	0.06	0.54	0.30	-0.24	0.27
	CRPSS	-0.40	-0.16	-0.05	0.19	0.09	0.01	-0.61
	PBIAS (%)	-10.01 *	-10.33 *	-14.41 *	-17.38 *	-17.22 *	-16.09 *	-11.28 *
	MAE (°C)	0.81 *	1.22 *	2.23 *	2.87 *	2.83 *	2.42 *	1.34 *
	RMSE (°C)	0.95	1.64	2.47	3.23	3.00	2.61	1.70
T_{min}	NRMSE (%)	11.78	14.85	17.26	19.57	18.23	17.85	14.89
	\mathbb{R}^2	0.71	0.31	0.00	0.06	0.01	0.20	0.00
	ACC	0.84 *	0.56	-0.03	0.24	-0.09	-0.44	0.03
	CRPSS	0.05	0.06	-0.92	-1.15	-2.59	-1.76	-0.39
	PBIAS (%)	3.43	3.59	-3.44	-5.56 *	-4.72 *	-3.42	3.76
	$MAE (^{\circ}C)$	0.70 *	1.37 *	1.63 *	1.91 *	1.44 *	1.28 *	1.08 *
	RMSE (°C)	0.88	1.57	1.82	2.27	1.73	1.54	1.48
T_{mean}	NRMSE (%)	5.83	8.17	7.93	8.66	6.60	6.68	7.81
	\mathbb{R}^2	0.62	0.42	0.00	0.10	0.01	0.05	0.06
	ACC	0.79 *	0.65 *	-0.04	0.32	-0.08	-0.22	0.24
	CRPSS	0.28	0.25	-0.13	-0.07	-0.34	-0.03	0.08

^{*} PBIAS, MAE, ACC statistical significance ($\alpha = 0.05$).

When analysing the correlation and anomaly prediction capability (ACC) results, a significant decline in performance is evident, at a level of significance (α) of 0.05, from the third month onward (Table 4). A similar pattern is observed for forecast skill, as measured by CRPSS; however, this decline is more evident for T_{min} and T_{mean} . These results suggest that the raw T_{min} and T_{mean} forecasts are mostly useful for the first two lead months, with a sharp decline in performance thereafter. T_{max} forecast skill is somewhat erratic, demonstrating poor performance during the first three leading months and in the last month. Bento et al. [42] also reported a clear deterioration in the skill of SEAS5 temperature forecasts after the first month. However, it is noteworthy that, in this study, the seventh month does not perform the worst performing month across all metrics or variables. This supports the idea that other factors can play a significant role in forecast performance beyond the simple effect of lead time.

It should be noted that this analysis is based on raw SWF extracted from a single grid point in the dataset and only considers one initialization month (April). A more extensive spatial and temporal analysis would be necessary to gain a clearer insight into the degradation of forecast performance with lead time. Furthermore, using post-processing techniques, such as bias correction or statistical downscaling, could significantly improve forecast accuracy and potentially extend the temporal range of time over which forecasts are useful. Therefore, these results should be interpreted as a preliminary assessment of raw forecast performance, highlighting the limitations and potential for refinement. However, these issues are beyond the scope of the current study.

3.2.2. Seasonal Validation

Figure 5 shows the results comparing seasonal temperature values from the reanalysis with those from the SWF. The results show that the mean forecast ensemble temperature data are in good agreement with the reanalysis, with no clear tendency to over- or underestimate the T_{mean} along the considered period. However, the accuracy and skill

indicators of the forecast data (Table 5), show that the T_{max} forecast slightly underestimates the reanalysis data, while the T_{min} forecast strongly overestimates them, as reported by other studies (e.g., [94]). These opposing biases tend to cancel each other out, reducing the overall error in estimating T_{mean} (Figure 5). The results indicate that the forecasts are more accurate in estimating T_{mean} than T_{max} and T_{min} , although a slight overestimation of T_{mean} remains (Table 5). Nevertheless, the error and bias are significant for all variables at the 95% confidence level (Table 5).

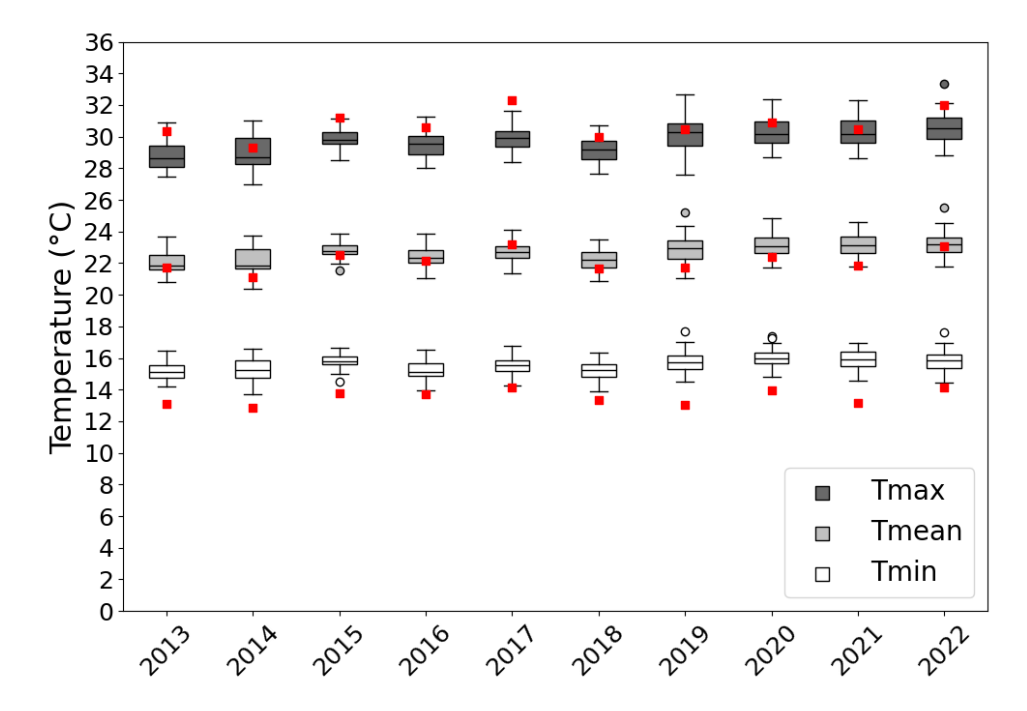


Figure 5. Box and whisker plots representing seasonal forecast ensemble of temperature data for April–September mean maximum (T_{max}) , minimum (T_{min}) , and mean (T_{mean}) temperatures, with dots and red squares representing the reanalysis mean of the temperature data.

Table 5. Temperature seasonal forecast accuracy and skill assessment.

Variable	PBIAS	\mathbb{R}^2	MAE	RMSE	NRMSE	ACC	CRPSS
T _{max}	3.48 *	0.44	1.07 *	1.25	4.05	0.66 *	-0.30
T_{min}	-15.01 *	0.16	2.03 *	2.08	15.36	0.40	-4.33
T_{mean}	-2.17 *	0.38	0.57 *	0.70	3.17	0.61	0.06

^{*} PBIAS, MAE, ACC statistical significance ($\alpha = 0.05$).

There is a considerable variation in the temperature bias of SWF, depending on the forecast model, season and region. There is no consensus in the literature as some studies report overestimation and others report underestimation. Many studies report that SWF tends to underestimate temperatures. For example, Renan et al. [95] found a cold bias in WRF model simulations applied to New Zealand, particularly during the southern hemisphere summer. Similarly, Ji et al. [96] reported that the WRF model systematically underestimated temperatures in Australia (by 2–3 °C for T_{max} and 1–2 °C for T_{min}). Ferreira et al. [97] reported a cold bias in SEAS5 for South America. Furthermore, studies in central and southern Europe [17,35,38,39,98] also reported a general underestimation of temperature by seasonal forecasting systems. However, in the present study, the significant overestimation of T_{min} prevented a general underestimation of T_{mean} .

The results also show that the SWF model is more accurate and skilful in forecasting T_{max} than T_{min} , as evidenced by lower estimation errors and higher R^2 values (Table 5).

However, the ensemble amplitude, which represents forecast uncertainty, is greater for T_{max} than for T_{min} (Figure 5).

There was a satisfactory agreement between the SWF anomalies and those of the reanalysis, with ACC > 0.40 (Table 5). This is especially true in the case of T_{max} , where there is agreement with a significance level of 0.05. Furthermore, the SWF skill assessed with the SAI (Figure 6) supports these findings, suggesting that the anomaly signal was accurately captured by the forecasts in 80% of the years for T_{max} , 60% for T_{min} , and 70% for T_{mean} . Patterson et al. [99] reported good agreement when analysing the summer temperature anomalies in Europe. In contrast, Calì Quaglia et al. [47] reported a negative ACC for winter and a slightly positive value for summer for Portugal using ECMWF seasonal forecasts.

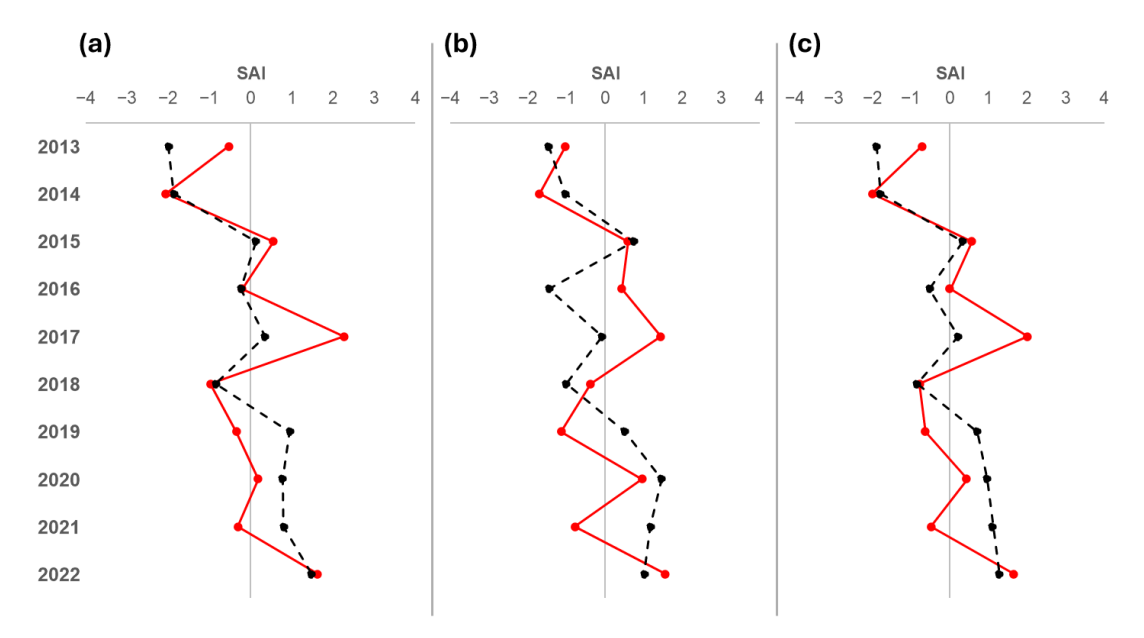


Figure 6. Standardised anomaly index (SAI) of temperature over the 2013–2022 period. Black-dashed lines represent SWF estimates; red solid lines correspond to reanalysis-based values. (a) T_{max} ; (b) T_{min} ; (c) T_{mean} .

Analysis of the results for the other skill indicator, CRPSS, shows that using SWF data does not provide a significant advantage over the historical average (Table 5). In fact, for T_{min} , the forecasts are considerably worse than the historical baseline. T_{mean} is the only variable with a positive CRPSS; however, all the values of the CRPSS are close to zero, indicating that temperature forecasts provide no meaningful added value compared to the historical average.

3.3. Seasonal Forecast Indirect Validation

Figure 7 shows the results of comparing forecasted and observed (reanalysis) crop cycle duration estimates using the GDD approach (Equation (2)), highlighting key trends and anomalies and reflecting the sensitivity of crop cycle duration estimation to temperature biases in the input data. Table 6 summarises the results of the accuracy and skill indicators used to assess the SWF ability to predict the crop cycle of the selected crops over the 10-year period (2013–2022). The results show that temperature forecasts cannot perfectly replicate the effects of climatic variability during the crop cycle.

Following the results of the SWF T_{mean} overestimation (Table 5), the results show that, overall, the forecasted crop cycles do not differ substantially from the reference (reanalysis) values but tend to underestimate the cycle duration (positive PBIAS) (Table 6). Notwithstanding, the error and bias are significant ($\alpha = 0.05$); on average, the underestimation is about one week (i.e., MAE ranging from 4.8 to 8.5 days). Lower accuracy was reported

in the study by Yang et al. [36] when using ECMWF SEAS5 forecasts to simulate the phenological development of vineyards in Portugal, with a potential forecast error of up to two weeks and an overall moderate forecast skill. Conversely, Garcia et al. [35] reported that WRF-based seasonal forecasts could lead to significant overestimates, with maize crop cycles in Portugal being extended by up to 60 days due to significant temperature underestimation by the SWF. Similar overestimates were also reported in the same study for wheat and maize in France and Greece. The error obtained in the current study, i.e., one week, can be considered adequate for supporting farmers' decision-making, particularly since the information is made available at the start of the season, i.e., seven months ahead. This level of estimation error is comparable to that obtained using Earth observation methods to retrieve crop growth stages from vegetation index time series. This is considered one of the most accurate approaches currently available for characterising the crop cycle as the accuracy is limited by the satellite revisit time [100,101]. Thus, the near real-time support also presents lags.

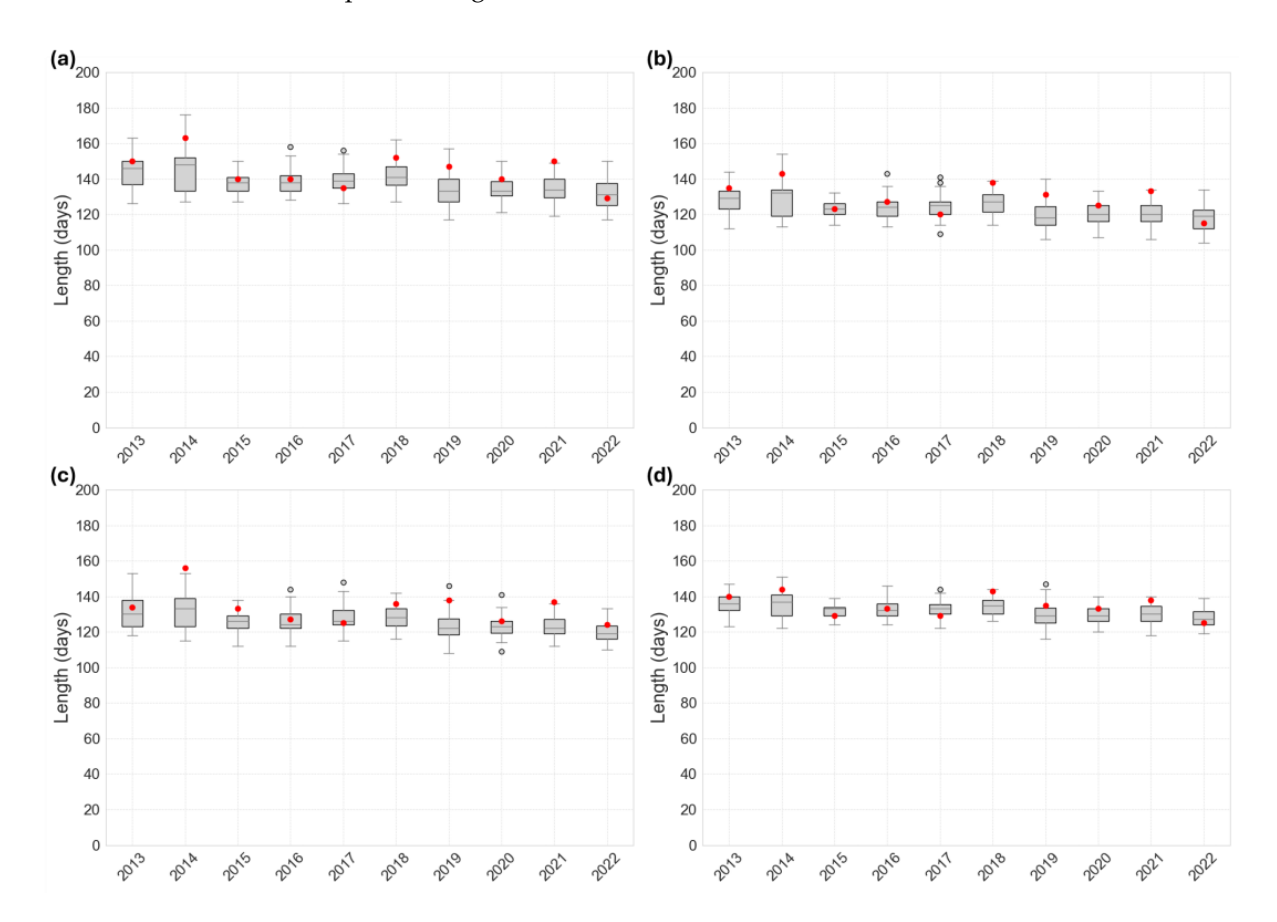


Figure 7. Box and whisker plots for the crop cycle duration when estimated using the seasonal forecasts and the reanalysis (red dots) for: (a) maize; (b) melon; (c) sunflower; (d) tomato.

Table 6. Seasonal forecast accuracy and skill assessment for the crop cycle duration estimation of selected cereal and vegetable crops, during 2013–2022 at the Caia Irrigation Scheme.

Crop	PBIAS (%)	R ²	MAE (Days)	RMSE (Days)	NRMSE (%)	ACC	CRPSS
Maize	4.5 *	0.46	7.70 *	9.44	6.5	0.68 *	0.15
Melon	4.1 *	0.39	7.10 *	8.31	6.4	0.63	0.16
Sunflower	6.2 *	0.43	8.50 *	10.88	8.1	0.66 *	-0.08
Tomato	2.1	0.46	4.80 *	5.31	3.9	0.67 *	0.26

^{*} PBIAS, MAE, ACC statistical significance ($\alpha = 0.05$).

Agronomy **2025**, 15, 1291 15 of 23

The results for the colder year of the data series (2014) indicate longer crop cycles for all crops. Although the ensemble did not capture the observed value within the interquartile range around the median value, it was able to capture the variability with a wider spread compared to other years. In this year, both the ensemble range and the maximum value were higher, indicating that the seasonal forecasting system was sensitive to some extent to the uncertainty associated with the atypical weather conditions and the nature of the anomaly.

Over the 10-year period, a general trend towards shorter crop cycles is observed (Figure 7), due to the tendency of T_{mean} to increase, as Espírito Santo et al. [102] reported for Portugal. Various studies confirm this global warming trend [103,104], which significantly impacts the shortening of crop cycles and, consequently, crop yields [25,58,105]. The forecasts effectively capture this trend, and the signal of anomalies are significantly correlated, as indicated by the ACC and SAI metrics (Table 6 and Figure 8). Therefore, these results demonstrate the potential of using SWF to predict crop growth cycles in advance when considering the observed climate trends in the region studied. This renders studies using fixed dates or tabulated crop cycle lengths outdated.

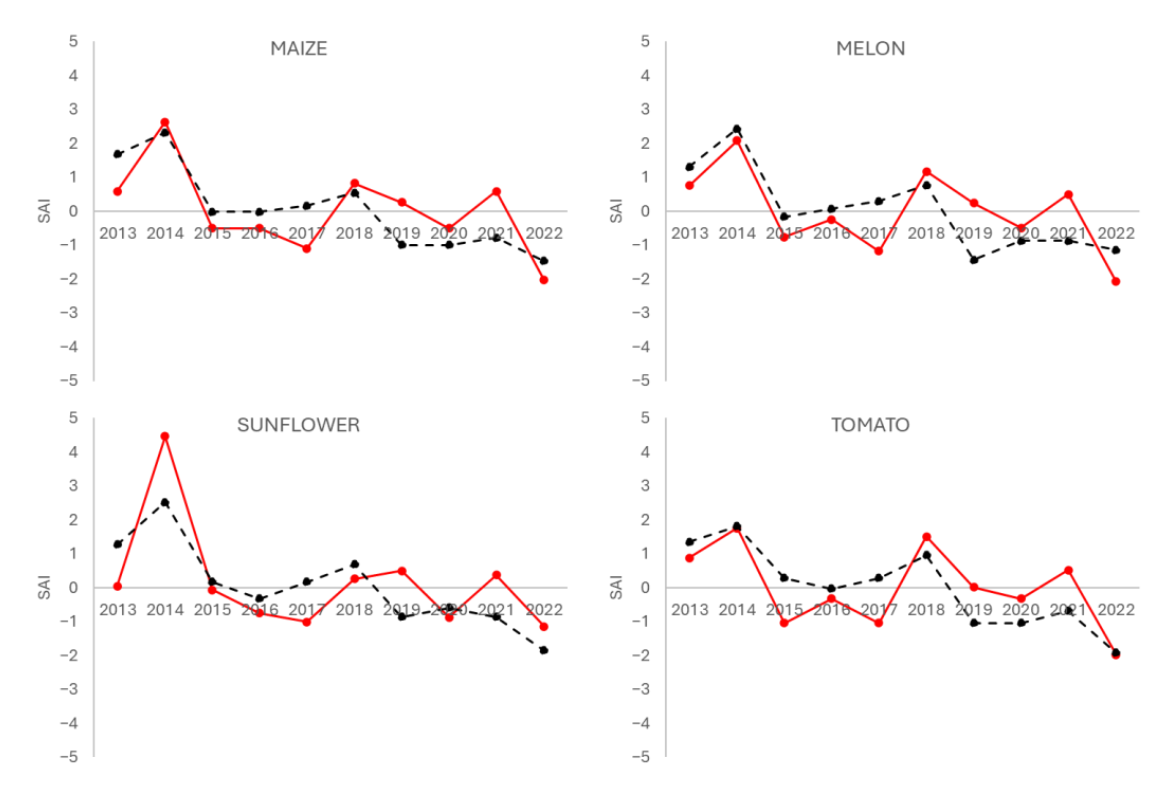


Figure 8. Standardised anomaly index (SAI) of crop cycle duration for maize, melon, sunflower, and tomato, over the 2013–2022 period in the Caia Irrigation Scheme. Black-dashed lines represent SWF estimates; red solid lines correspond to reanalysis-based values.

It is important to note that the CRPSS values were positive for three of the four selected crops (Table 6). These results suggest that the ECMWF SEAS5 seasonal temperature forecasts have a reasonable skill and advantage over the historical average at estimating crop cycle duration for the selected crops in the CIS, except for sunflower, for which the CRPSS value was negative, but close to zero (Table 6).

In addition to assessing the ability of the SWF to estimate crop cycle duration by replicating climate variability, the accuracy of estimating the length of crop cycles was also evaluated, taking into account the variability in crop conditions from one year to the next, over the 2017–2019 period. Analysis of Table 7 shows that difference in estimated crop cycle length between the SWF and the AgERA5 data ranged from -12 to 4 days for maize,

from -11 to 5 days for melon, from -7 to 1 days for sunflower and -6 to 4 days for tomato. Overall, the SWF once again presents a mean difference of around one week (see Table 6). This is within the range of variation in crop cycle duration observed using satellite data. As shown in Table 1, there is considerable variability in GDD values and cycle lengths across the various years (2017–2019), reflecting differences in both climatic conditions and agronomic practices. Therefore, it can be stated that the SWF has great potential to reduce the errors introduced by using tabulated/fixed crop cycles values, which can be inaccurate by several weeks. This error is lower than the deviations that can result due to the use of different cultivars, or to the use of diverse cultural practices, thus providing good prospects for the use of SWF to support farmers' decision-making.

Table 7. Difference in crop cycle length derived from NDVI satellite data, reanalysis AgERA5 data
and SEAS5 seasonal forecast data (SF) (2017–2019).

Crop	Year	Length	Length AgERA5	Length SF	Difference (SF-AgERA5)		
	2017	137	135	139	4		
Maize	2018	128	128	117	-11		
	2019	150	148	136	-12		
	2017	122	120	125	5		
Melon	2018	Not available					
	2019	107	105	94	-11		
	2017	127	125	126	1		
Sunflower	2018	118	118	109	-9		
	2019	122	120	113	-7		
	2017	130	129	133	4		
Tomato	2018		Not a	vailable			
	2019	132	130	124	-6		

4. Conclusions

This study highlights the potential of integrating ground-based observations, Earth observation data, reanalysis datasets and SWF data into GDD tools to support agricultural decision-making under climate variability. The results show that the bias-corrected AgERA5 reanalysis datasets offer accurate temperature estimates, enabling effective upscaling from point (weather station) measurements to irrigation system scale.

Evaluating the ECMWF SEAS5 raw seasonal forecasts (seven months) showed persistent temperature biases, with a tendency to underestimate T_{max} and overestimate T_{min} , but with small errors in the estimates of approximately 1 °C and 2 °C, respectively. These opposite errors partially offset each other, resulting in improved estimates of T_{mean} ; however, a slight overestimation was observed. When applying the GDD approach, these temperature biases affected accumulation, leading to a consistent underestimation of crop cycle duration for the spring—summer crops of around eight days for maize, seven days for melon, nine days for sunflower and five days for tomato.

Forecast skill declined non-linearly with lead time, particularly beyond the second month, reflecting the influence of seasonal climate variability. However, the forecasts captured important signals, such as the general warming trend over the period 2013–2022 and interannual variability, particularly for T_{max} and T_{mean} . Skill metrics, including ACC, SAI and CRPSS, indicated that the raw SWF provided marginal added value over historical climatology for most crops.

Overall, the results support the use of uncorrected (raw) seasonal temperature forecasts to inform early season planning and adaptive management practices, such as adjusting

planting and harvesting schedules or fertiliser management. Integrating these forecasts into GDD-based decision-support tools could contribute to more informed decisions, promoting yield optimisation and improving the efficiency with which resources are used, particularly water, in water-scarce agricultural regions. Although the presented methodology can be transferred and applied to other regions, the specific results depend on local agro-climatic conditions and should therefore be interpreted in the context of the targeted region. Future work should focus on applying different bias correction methods and further validating the SWF at broader spatial and temporal scales, with the aim of improving its operational value in climate-resilient agriculture.

Author Contributions: Conceptualization, D.G. and P.P.; Methodology, D.G. and P.P.; Software, D.G., N.S. and A.F.; Validation, D.G. and N.S.; Formal analysis, D.G., N.S., A.F. and P.P.; Investigation, J.R. and P.P.; Resources, D.G. and A.F.; Data curation, D.G. and A.F.; Writing—original draft, D.G. and N.S.; Writing—review & editing, D.G., J.R., A.F., J.A.S., M.d.R.C. and P.P.; Visualization, D.G. and N.S.; Supervision, J.R., J.A.S. and P.P.; Project administration, P.P.; Funding acquisition, P.P. All authors have read and agreed to the published version of the manuscript.

Funding: This research was funded by FCT—Fundação para a Ciência e a Tecnologia, I.P., through the project WaterQB 2022.04553.PTDC (https://doi.org/10.54499/2022.04553.PTDC).

Data Availability Statement: The data presented in this study are available on request from the corresponding authors.

Acknowledgments: The support of FCT—Fundação para a Ciência e a Tecnologia, I.P., under the projects WaterQB 2022.04553.PTDC (https://doi.org/10.54499/2022.04553.PTDC), UIDB/04129/2020 of LEAF-Linking Landscape, Environment, Agriculture and Food, Research Unit, LA/P/0092/2020 of Associate Laboratory TERRA, Centre for the Research and Technology of Agro-Environmental and Biological Sciences CITAB (UID/04033, (https://doi.org/10.54499/UIDB/04033/2020) and Associate Laboratory Inov4Agro (LA/P/0126/2020, https://doi.org/10.54499/LA/P/0126/2020) are also acknowledged.

Conflicts of Interest: The authors declare no conflicts of interest.

Appendix A

Table A1. Performance Metrics for Seasonal Forecast Evaluation.

Indicator	Equation	Description
Bias Percentage (PBIAS)	$100 \times \frac{\sum_{i}^{n}(R_{i}-F_{i})}{\sum_{i=1}^{n}R_{i}}$	R_i is the reanalysis based value, F_i is the seasonal forecast based value, in the year i, and n is the number of years. Quantifies the average tendency of the forecast data to overestimate or underestimate the reference values. Positive values indicate forecast underestimation, while negative values indicate forecast overestimation. Deterministic approach using the forecast ensemble median.
Coefficient of Determination (R^2)	$\frac{\sum_{i=1}^{n} \left(\hat{F}_{i} - \overline{F}\right)^{2}}{\sum_{i=1}^{n} \left(F_{i} - \overline{F}\right)^{2}}$	F_i is the seasonal forecast based value, in the year i, and n is the number of years, \hat{F}_i is the regression line adjusted forecast based value, \overline{F} is the mean of forecast based values. Measures the proportion of variance in the reanalysis values explained by the forecast model. Ranges from 0 to 1. Higher R^2 values indicate that a large proportion of the variance in reanalysis values is explained by the forecasts. Deterministic approach using the forecast ensemble median.

 Table A1. Cont.

Indicator	Equation	Description
Mean Absolute Error (MAE)	$rac{\sum_{i=1}^{n} F_{i}-R_{i} }{n}$	R_i is the reanalysis based value, F_i is the seasonal forecast based value, in the year i, and n is the number of years. Measures the average magnitude of errors between forecasts and reference values, without considering their direction. Lower values indicate better accuracy. Deterministic approach using the forecast ensemble median.
Root Mean Square Error (RMSE)	$\sqrt{\frac{\sum_{i=1}^{n}{(R_i - F_i)^2}}{n}}$	R_i is the reanalysis based value, F_i is the seasonal forecast based value, in the year i, and n is the number of years. Measures the square root of the average squared differences between forecasts and reference values. Penalises larger errors more than MAE. Deterministic approach using the forecast ensemble median.
Normalised Root Mean Square Error (NRMSE)	$100 \times \frac{\text{RMSE}}{\overline{R}}$	\overline{R} is the mean of reanalysis based values. Provides a dimensionless measure of the model's relative error. Useful for comparing performance across variables or scales. Deterministic approach using the forecast ensemble median.
Standardised Anomaly Index (SAI)	$\frac{T-T_c}{\sigma}$	T is the mean seasonal temperature mean for a given year, T_c is the long-term (2013–2022) mean seasonal temperature, and σ is the standard deviation of the seasonal temperature mean for the long-term dataset. Measures the standardised anomaly of seasonal temperature. Indicates how many standard deviations the seasonal value deviates from the long-term mean. Deterministic approach using the forecast ensemble median.
Anomaly Correlation Coefficient (ACC)	$\frac{\frac{\sum_{i=1}^{n} \ (F_i - F_c) \left(R_i - R_c\right)}{n}}{\sqrt{\frac{\sum_{i=1}^{n} \left(\frac{F_i - F_c}{n}\right)^2}{n} \cdot \frac{\sum_{i=1}^{n} \left(\frac{R_i - R_c}{n}\right)}{n}}}$	R_i is the reanalysis based value, R_c the is the long-term (2013–2022) reanalysis mean, F_i is the seasonal forecast based value, F_c is the long-term forecast mean, in the year i, and n is the number of years. Measures the correlation between forecast anomalies and observed anomalies. Ranges from -1 to 1, with positive values indicating agreement between forecast and reanalysis anomalies. Reanalysis anomalies were calculated relative to the 10-year reanalysis dataset, while the forecast anomalies were calculated relative to the 10-year forecast dataset. Deterministic approach using the forecast ensemble median.
Continuous Ranked Probability Skill Score (CRPSS)	$1 - \frac{\text{CRPS}_F}{\text{CRPS}_R}$	CRPS _F and CRPS _R are the continuous ranked probability score for the forecast and the reanalysis, respectively. Quantifies the skill of the forecast in relation to the reanalysis based climatology. A CRPSS of 1 means a perfect forecast, 0 means the forecast is as good as the reanalysis historical average, and negative values indicate worse skill than the long-term average. This analysis was performed using the SeaVal: Validation of Seasonal Weather Forecasts R package. Probabilistic approach using all the forecast ensemble members.

References

1. Zou, Z.; Li, C.; Wu, X.D.; Zheng, M.; Cheng, C. The Effect of Day-to-Day Temperature Variability on Agricultural Productivity. *Environ. Res. Lett.* **2024**, *19*, 124046. [CrossRef]

- 2. Minoli, S.; Jägermeyr, J.; Asseng, S.; Urfels, A.; Müller, C. Global Crop Yields Can Be Lifted by Timely Adaptation of Growing Periods to Climate Change. *Nat. Commun.* **2022**, *13*, 7079. [CrossRef] [PubMed]
- 3. Kummu, M.; Heino, M.; Taka, M.; Varis, O.; Viviroli, D. Climate Change Risks Pushing One-Third of Global Food Production Outside the Safe Climatic Space. *One Earth* **2021**, *4*, 720–729. [CrossRef]
- 4. Zhu, P.; Burney, J.; Chang, J.; Jin, Z.; Mueller, N.; Xin, Q.; Xu, J.; Yu, L.; Makowski, D.; Ciais, P. Warming Reduces Global Agricultural Production by Decreasing Cropping Frequency and Yields. *Nat. Clim. Change* **2022**, *12*, 1016–1023. [CrossRef]
- 5. Ali, E.; Cramer, W.; Carnicer, J.; Georgopoulou, E.; Hilmi, N.J.M.; Le Cozannet, G.; Lionello, P. Cross-Chapter Paper 4: Mediterranean Region. In *Climate Change 2022: Impacts, Adaptation and Vulnerability*; Contribution of Working Group II to the Sixth Assessment Report of the Intergovernmental Panel on Climate, Change; Pörtner, H.-O., Roberts, D.C., Tignor, M., Poloczanska, E.S., Mintenbeck, K., Alegría, A., Craig, M., Langsdorf, S., Löschke, S., Möller, V., et al., Eds.; Cambridge University PressL: Cambridge, UK; New York, NY, USA, 2022; pp. 2233–2272. [CrossRef]
- 6. Drobinski, P.; Da Silva, N.; Bastin, S.; Mailler, S.; Muller, C.; Ahrens, B.; Christensen, O.; Lionello, P. How Warmer and Drier Will the Mediterranean Region Be at the End of the Twenty-First Century? *Reg. Environ. Change* **2020**, *20*, 78. [CrossRef]
- 7. Intergovernmental Panel On Climate Change (IPCC). Climate Change 2022—Impacts, Adaptation and Vulnerability: Working Group II Contribution to the Sixth Assessment Report of the Intergovernmental Panel on Climate Change; Pörtner, H.-O., Roberts, D.C., Tignor, M., Poloczanska, E.S., Mintenbeck, K., Alegría, A., Craig, M., Langsdorf, S., Löschke, S., Möller, V., et al., Eds.; Cambridge University Press: Cambridge, UK; New York, NY, USA, 2023; 3056p. [CrossRef]
- 8. Cramer, W.; Guiot, J.; Marini, K. (Eds.) Climate and Environmental Change in the Mediterranean Basin—Current Situation and Risks for the Future. First Mediterranean Assessment Report; Mediterranean Experts on Climate and Environmental Change, Union for the Mediterranean, Plan Bleu, UNEP/MAP: Marseille, France, 2020; 632p. [CrossRef]
- 9. Webber, H.; Lischeid, G.; Sommer, M.; Finger, R.; Nendel, C.; Gaiser, T.; Ewert, F. No Perfect Storm for Crop Yield Failure in Germany. *Environ. Res. Lett.* **2020**, *15*, 104012. [CrossRef]
- 10. Menzel, A.; Yuan, Y.; Matiu, M.; Sparks, T.; Scheifinger, H.; Gehrig, R.; Estrella, N. Climate Change Fingerprints in Recent European Plant Phenology. *Glob. Chang. Biol.* **2020**, *26*, 2599–2612. [CrossRef]
- 11. Rezaei, E.; Webber, H.; Asseng, S.; Boote, K.; Durand, J.-L.; Ewert, F.; Martre, P.; Maccarthy, D. Climate Change Impacts on Crop Yields. *Nat. Rev. Earth Environ.* **2023**, *4*, 831–846. [CrossRef]
- 12. Kukal, M.S.; Irmak, S. Climate-Driven Crop Yield and Yield Variability and Climate Change Impacts on the U.S. Great Plains Agricultural Production. *Sci. Rep.* **2018**, *8*, 3450. [CrossRef]
- 13. Auci, S.; Vignani, D. Climate Variability and Agriculture in Italy: A Stochastic Frontier Analysis at the Regional Level. *Econ. Politica* **2020**, *37*, 381–409. [CrossRef]
- 14. Yuan, X.; Li, S.; Chen, J.; Yu, H.; Tianyi, Y.; Wang, C.; Huang, S.; Haochong, C.; Ao, X. Impacts of Global Climate Change on Agricultural Production: A Comprehensive Review. *Agronomy* **2024**, *14*, 1360. [CrossRef]
- 15. Dainelli, R.; Calmanti, S.; Pasqui, M.; Rocchi, L.; Di Giuseppe, E.; Monotti, C.; Quaresima, S.; Matese, A.; Di Gennaro, S.; Toscano, P. Moving Climate Seasonal Forecasts Information from Useful to Usable for Early Within-Season Predictions of Durum Wheat Yield. Clim. Serv. 2022, 28, 100324. [CrossRef]
- 16. Rodriguez, D.; de Voil, P.; Hudson, D.; Brown, J.; Hayman, P.; Marrou, H.; Meinke, H. Predicting Optimum Crop Designs Using Crop Models and Seasonal Climate Forecasts. *Sci. Rep.* **2018**, *8*, 2231. [CrossRef]
- 17. Villani, G.; Tomei, F.; Pavan, V.; Pirola, A.; Spisni, A.; Marletto, V. The ICOLT Climate Service: Seasonal Predictions of Irrigation for Emilia-Romagna, Italy. *Meteorol. Appl.* **2021**, *28*, 2007. [CrossRef]
- 18. Chen, Y.; Tao, F. Potential of Remote Sensing Data-Crop Model Assimilation and Seasonal Weather Forecasts for Early-Season Crop Yield Forecasting over a Large Area. *Field Crops Res.* **2022**, *276*, 108398. [CrossRef]
- 19. Fleming, A.; Fielke, S.; Jakku, E.; Malakar, Y.; Snow, S.; Clarry, S.; Tozer, C.; Darbyshire, R.; Legge, D.; Samson, A.; et al. Developing Climate Services for Use in Agricultural Decision Making: Insights from Australia. *Clim. Serv.* 2025, 37, 100537. [CrossRef]
- 20. Ritchie, J.T.; NeSmith, D.S. Temperature and Crop Development. In *Modeling Plant and Soil Systems*; Hanks, R.J., Ritchie, J.T., Eds.; Agronomy Monographs 31; American Society of Agronomy: Madison, WI, USA, 1991; pp. 5–29.
- 21. Bonhomme, R. Bases and Limits to Using 'Degree.Day' Units. Eur. J. Agron. 2000, 13, 1–10. [CrossRef]
- 22. Roth, L.; Binder, M.; Kirchgessner, N.; Tschurr, F.; Yates, S.; Hund, A.; Kronenberg, L.; Walter, A. From Neglecting to Including Cultivar-Specific Per Se Temperature Responses: Extending the Concept of Thermal Time in Field Crops. *Plant Phenomics* 2025, 6, 0185. [CrossRef]
- 23. Yang, C.; Lei, N.; Menz, C.; Ceglar, A.; Torres-Matallana, J.A.; Li, S.; Jiang, Y.; Tan, X.; Tao, L.; He, F.; et al. Regional Uncertainty Analysis between Crop Phenology Model Structures and Optimal Parameters. *Agric. Meteorol.* **2024**, *355*, 110137. [CrossRef]

Agronomy **2025**, 15, 1291 20 of 23

24. Jagadish, S.V.K.; Bahuguna, R.N.; Djanaguiraman, M.; Gamuyao, R.; Prasad, P.V.V.; Craufurd, P.Q. Implications of High Temperature and Elevated CO2 on Flowering Time in Plants. *Front. Plant Sci.* **2016**, 7, 2016. [CrossRef]

- 25. Zhao, C.; Liu, B.; Piao, S.; Wang, X.; Lobell, D.; Huang, Y.; Huang, M.; Yao, Y.; Bassu, S.; Ciais, P.; et al. Temperature Increase Reduces Global Yields of Major Crops in Four Independent Estimates. *Proc. Natl. Acad. Sci. USA* 2017, 114, 201701762. [CrossRef] [PubMed]
- 26. Wang, J.Y. A Critique of the Heat Unit Approach to Plant Response Studies. Ecology 1960, 41, 785–790. [CrossRef]
- 27. McMaster, G.S.; Wilhelm, W.W. Growing Degree-Days: One Equation, Two Interpretations. *Agric. Meteorol.* **1997**, *87*, 291–300. [CrossRef]
- 28. Salman, M.; García Vila, M.; Fereres, E.; Raes, D.; Steduto, P.; Heng, L.; De Lannoy, G.; Wellens, J.; Foster, T.; Busschaert, L.; et al. *AquaCrop on the Ground*; FAO Water Reports 48; FAO: Rome, Italy, 2025; 92p. [CrossRef]
- 29. Müller, C.; Elliott, J.; Chryssanthacopoulos, J.; Arneth, A.; Balkovic, J.; Ciais, P.; Deryng, D.; Folberth, C.; Glotter, M.; Hoek, S.; et al. Global Gridded Crop Model Evaluation: Benchmarking, Skills, Deficiencies And. *Geosci. Model. Dev.* 2017, 10, 1403–1422. [CrossRef]
- 30. Allen, R.; Robison, C.; Huntington, J.; Wright, J.; Kilic, A. Applying the FAO-56 Dual Kc Method for Irrigation Water Requirements over Large Areas of the Western U.S. *Trans. ASABE* **2020**, *63*, 2059–2081. [CrossRef]
- 31. Pearson, C.; Minor, B.A.; Morton, C.G.; Volk, J.M.; Dunkerly, C.W.; Jensen, E.; ReVelle, P.; Kilic, A.; Allen, R.; Huntington, J.L. Historical Evapotranspiration and Consumptive Use of Irrigated Areas of the Upper Colorado River Basin; DRI Report No. 41304; Desert Research Institute: Las Vegas, NV, USA, 2024. [CrossRef]
- 32. Johnson, S.J.; Stockdale, T.N.; Ferranti, L.; Balmaseda, M.A.; Molteni, F.; Magnusson, L.; Tietsche, S.; Decremer, D.; Weisheimer, A.; Balsamo, G.; et al. SEAS5: The New ECMWF Seasonal Forecast System. *Geosci. Model. Dev.* **2019**, 12, 1087–1117. [CrossRef]
- 33. Crespi, A.; Petitta, M.; Marson, P.; Viel, C.; Grigis, L. Verification and Bias Adjustment of ECMWF SEAS5 Seasonal Forecasts over Europe for Climate Service Applications. *Climate* **2021**, *9*, 181. [CrossRef]
- 34. Stockdale, T. SEAS5 User Guide; Version 1.2; ECMWF: Reading, UK, 2021; 24p. [CrossRef]
- 35. Garcia, D.; Rolim, J.; Cameira, M.d.R.; Belaud, G.; Dalezios, N.R.; Karoutsos, G.; Santos, J.A.; Paredes, P. Assessing Seasonal Forecast Performance to Predict Crop Irrigation Requirements to Support Water Management Decision-Making in the Mediterranean Region. *Agric. Water Manag.* 2025, 313, 109467. [CrossRef]
- 36. Yang, C.; Ceglar, A.; Menz, C.; Martins, J.; Fraga, H.; Santos, J. Performance of Seasonal Forecasts for the Flowering and Veraison of Two Major Portuguese Grapevine Varieties. *Agric. Meteorol.* **2023**, *331*, 109342. [CrossRef]
- 37. Capa-Morocho, M.; Ines, A.V.M.; Baethgen, W.E.; Rodríguez-Fonseca, B.; Han, E.; Ruiz-Ramos, M. Crop Yield Outlooks in the Iberian Peninsula: Connecting Seasonal Climate Forecasts with Crop Simulation Models. *Agric. Syst.* **2016**, *149*, 75–87. [CrossRef]
- 38. Lalic, B.; Firanj Sremac, A.; Dekic, L.; Eitzinger, J. Seasonal Forecasting of Green Water Components and Crop Yields of Winter Wheat in Serbia and Austria. *J. Agric. Sci.* **2017**, *156*, 1–17. [CrossRef]
- 39. Lalic, B.; Firanj Sremac, A.; Eitzinger, J.; Stricevic, R.; Thaler, S.; Maksimovic, I.; Danicic, M.; Dekic, L. Seasonal Forecasting of Green Water Components and Crop Yield of Summer Crops in Serbia and Austria. *J. Agric. Sci.* **2018**, *156*, 1–15. [CrossRef]
- 40. Velde, M.; Nisini, L. Performance of the MARS-Crop Yield Forecasting System for the European Union: Assessing Accuracy, in-Season, and Year-to-Year Improvements from 1993 to 2015. *Agric. Syst.* **2018**, *168*, 203–212. [CrossRef]
- 41. Santos, J.A.; Ceglar, A.; Toreti, A.; Prodhomme, C. Performance of Seasonal Forecasts of Douro and Port Wine Production. *Agric. Meteorol.* **2020**, *291*, 108095. [CrossRef]
- 42. Bento, V.A.; Russo, A.; Dutra, E.; Ribeiro, A.F.S.; Gouveia, C.M.; Trigo, R.M. Persistence versus Dynamical Seasonal Forecasts of Cereal Crop Yields. *Sci. Rep.* **2022**, *12*, 7422. [CrossRef]
- Ramírez-Rodrigues, M.; Alderman, P.; Stefanova, L.; Cossani, C.; Flores, D.; Asseng, S. The Value of Seasonal Forecasts for Irrigated, Supplementary Irrigated, And Rainfed Wheat Cropping Systems in Northwest Mexico. Agric. Syst. 2016, 147, 76–86.
 [CrossRef]
- 44. An-Vo, D.-A.; Mushtaq, S.; Reardon-Smith, K.; Kouadio, L.; Attard, S.; Cobon, D.; Stone, R. Value of Seasonal Forecasting for Sugarcane Farm Irrigation Planning. *Eur. J. Agron.* **2019**, *104*, 37–48. [CrossRef]
- 45. Vogel, E.; Lerat, J.; Pipunic, R.; Frost, A.J.; Donnelly, C.; Griffiths, M.; Hudson, D.; Loh, S. Seasonal Ensemble Forecasts for Soil Moisture, Evapotranspiration and Runoff across Australia. *J. Hydrol.* **2021**, *601*, 126620. [CrossRef]
- 46. Judt, F. Atmospheric Predictability of the Tropics, Middle Latitudes, and Polar Regions Explored Through Global Storm-Resolving Simulations. *J. Atmos. Sci.* **2019**, 77, 257–276. [CrossRef]
- 47. Calì Quaglia, F.; Silvia, T.; Hardenberg, J. Temperature and Precipitation Seasonal Forecasts over the Mediterranean Region: Added Value Compared to Simple Forecasting Methods. *Clim. Dyn.* **2021**, *58*, 2167–2191. [CrossRef]
- 48. Ceglar, A.; Toreti, A. Seasonal Climate Forecast Can Inform the European Agricultural Sector Well in Advance of Harvesting. *NPJ Clim. Atmos. Sci.* **2021**, *4*, 42. [CrossRef]

Agronomy **2025**, 15, 1291 21 of 23

49. Costa-Saura, J.M.; Mereu, V.; Santini, M.; Trabucco, A.; Spano, D.; Bacciu, V. Performances of Climatic Indicators from Seasonal Forecasts for Ecosystem Management: The Case of Central Europe and the Mediterranean. *Agric. Meteorol.* **2022**, *319*, 108921. [CrossRef]

- 50. Bruno Soares, M.; Dessai, S. Barriers and Enablers to the Use of Seasonal Climate Forecasts amongst Organisations in Europe. *Clim. Change* **2016**, 137, 89–103. [CrossRef] [PubMed]
- 51. Klemm, T.; McPherson, R. The Development of Seasonal Climate Forecasting for Agricultural Producers. *Agric. For. Meteorol.* **2017**, 232, 384–399. [CrossRef]
- 52. Ferreira, A.; Rolim, J.; Paredes, P.; Cameira, M. do R. Assessing Spatio-Temporal Dynamics of Deep Percolation Using Crop Evapotranspiration Derived from Earth Observations through Google Earth Engine. *Water* **2022**, *14*, 2324. [CrossRef]
- 53. Instituto Nacional de Estatística (INE). Estatísticas Agrícolas 2023. Lisboa, Portugal: Instituto Nacional de Estatística. 2024. Available online: https://www.ine.pt/ (accessed on 3 April 2025).
- 54. FAO. International Soil Classification System for Naming Soils and Creating Legends for Soil Maps. In *World Reference Base for Soil Resources*; FAO: Roma, Italy, 2014.
- 55. Nunes, J.M.R. Los Suelos del Perímetro Regable del Caia (Portugal): Tipos, Fertilidade, e Impacto del Riego en sus Propriedades Químicas. Ph.D. Thesis, Universidad de Extremadura, Faculdad de Ciencias, Badajoz, Spain, 2013.
- 56. Beck, H.E.; Zimmermann, N.E.; McVicar, T.R.; Vergopolan, N.; Berg, A.; Wood, E.F. Present and Future Köppen-Geiger Climate Classification Maps at 1-Km Resolution. *Sci. Data* **2018**, *5*, 180214. [CrossRef]
- 57. Paulo, A.; Rosa, R.; Pereira, L. Climate Trends and Behaviour of Drought Indices Based on Precipitation and Evapotranspiration in Portugal. *Nat. Hazards Earth Syst. Sci.* **2012**, 12, 1481–1491. [CrossRef]
- 58. Yang, C.; Fraga, H.; van Ieperen, W.; Santos, J.A. Assessing the Impacts of Recent-Past Climatic Constraints on Potential Wheat Yield and Adaptation Options under Mediterranean Climate in Southern Portugal. *Agric. Syst.* **2020**, *182*, 102844. [CrossRef]
- 59. Oliveira, I.; Maia, J.; Teixeira, J.L. O sistema agrometeorológico para a gestão da rega no Alentejo—Sagra como serviço de avisos de rega para o Alentejo. In Proceedings of the 7° Congresso da Água Associação Portuguesa Dos Recursos Hídricos, Lisboa, Portugal, 8–12 March 2024; 2004; pp. 1–23. Available online: https://www.aprh.pt/congressoagua2004/PDF/22.PDF (accessed on 1 March 2025).
- 60. Boogaard, H.; Schubert, J.; De Wit, A.; Lazebnik, J.; Hutjes, R.; Van der Grijn, G. Agrometeorological indicators from 1979 to present derived from reanalysis. *Copernic. Clim. Change Serv. C3S Clim. Data Store CDS* **2020**. [CrossRef]
- Araghi, A.; Jaghargh, M.R.; Maghrebi, M.; Martinez, C.J.; Fraisse, C.W.; Olesen, J.E.; Hoogenboom, G. Investigation of Satellite-Related Precipitation Products for Modeling of Rainfed Wheat Production Systems. *Agric. Water Manag.* 2021, 258, 107222.
 [CrossRef]
- 62. Soulis, K.; Dosiadis, E.; Nikitakis, E.; Charalambopoulos, I.; Kairis, O.; Katsogiannou, A.; Palli Gravani, S.; Kalivas, D. Assessing AgERA5 and MERRA-2 Global Climate Datasets for Small-Scale Agricultural Applications. *Atmosphere* 2025, 16, 263. [CrossRef]
- 63. Paredes, P.; Martins, D.S.; Pereira, L.S.; Cadima, J.; Pires, C. Accuracy of Daily Estimation of Grass Reference Evapotranspiration Using ERA-Interim Reanalysis Products with Assessment of Alternative Bias Correction Schemes. *Agric. Water Manag.* **2018**, 210, 340–353. [CrossRef]
- 64. Cardoso, R.M.; Soares, P.M.M. Is There Added Value in the EURO-CORDEX Hindcast Temperature Simulations? Assessing the Added Value Using Climate Distributions in Europe. *Int. J. Climatol.* **2022**, 42, 4024–4039. [CrossRef]
- 65. Sebbar, B.; Khabba, S.; Merlin, O.; Simonneaux, V.; El Hachimi, C.; Kharrou, M.H.; Chehbouni, A. Machine-Learning-Based Downscaling of Hourly ERA5-Land Air Temperature over Mountainous Regions. *Atmosphere* **2023**, *14*, 610. [CrossRef]
- Copernicus Climate Change Service; Climate Data Store. Seasonal forecast daily and subdaily data on single levels. Copernic. Clim. Chang. Serv. C3S Clim. Data Store CDS 2018. [CrossRef]
- 67. Allen, R. Quality Assessment of Weather Data and Micrometeological Flux—Impacts on Evapotranspiration Calculation. *J. Agric. Meteorol.* **2008**, *64*, 191–204. [CrossRef]
- 68. Pereira, L.S.; Allen, R.; Paredes, P.; Smith, M.; Raes, D.; Kilic, A.; Salman, M. *Crop Evapotranspiration*; Guidelines for Computing Crop Water Requirements; FAO Irrigation & Drainage paper 56rev: Rome, Italy, 2025; *in press*.
- 69. Pelosi, A.; Medina, H.; Van den Bergh, J.; Vannitsem, S.; Chirico, G.B. Adaptive Kalman Filtering for Postprocessing Ensemble Numerical Weather Predictions. *Mon. Weather Rev.* **2017**, *145*, 4837–4854. [CrossRef]
- 70. Pelosi, A.; Terribile, F.; D'Urso, G.; Chirico, G.B. Comparison of ERA5-Land and UERRA MESCAN-SURFEX Reanalysis Data with Spatially Interpolated Weather Observations for the Regional Assessment of Reference Evapotranspiration. *Water* 2020, 12, 1669. [CrossRef]
- 71. Paredes, P.; Trigo, I.; de Bruin, H.; Simões, N.; Pereira, L.S. Daily Grass Reference Evapotranspiration with Meteosat Second Generation Shortwave Radiation and Reference ET Products. *Agric. Water Manag.* **2021**, 248, 106543. [CrossRef]
- Zhou, L.; Chen, H.; Xu, L.; Cai, R.-H.; Chen, D. Deep Learning-Based Postprocessing for Hourly Temperature Forecasting. Meteorol. Appl. 2024, 31, e2194. [CrossRef]

73. Dunkerly, C.; Huntington, J.; McEvoy, D.; Morway, A.; Allen, R. Agweather-Qaqc: An Interactive Python Package for Quality Assurance and Quality Control of Daily Agricultural Weather Data and Calculation of Reference Evapotranspiration. *J. Open Source Softw.* 2024, *9*, 6368. [CrossRef]

- 74. Nash, J.E.; Sutcliffe, J. V River Flow Forecasting through Conceptual Models Part I—A Discussion of Principles. *J. Hydrol. Amst* 1970, 10, 282–290. [CrossRef]
- 75. Pelosi, A.; Chirico, G.B. Regional Assessment of Daily Reference Evapotranspiration: Can Ground Observations Be Replaced by Blending ERA5-Land Meteorological Reanalysis and CM-SAF Satellite-Based Radiation Data? *Agric. Water Manag.* **2021**, 258, 107169. [CrossRef]
- 76. Vanella, D.; Longo-Minnolo, G.; Belfiore, O.R.; Ramírez-Cuesta, J.M.; Pappalardo, S.; Consoli, S.; D'Urso, G.; Chirico, G.B.; Coppola, A.; Comegna, A.; et al. Comparing the Use of ERA5 Reanalysis Dataset and Ground-Based Agrometeorological Data under Different Climates and Topography in Italy. *J. Hydrol. Reg. Stud.* 2022, 42, 101182. [CrossRef]
- 77. Ippolito, M.; De Caro, D.; Cannarozzo, M.; Provenzano, G.; Ciraolo, G. Evaluation of Daily Crop Reference Evapotranspiration and Sensitivity Analysis of FAO Penman-Monteith Equation Using ERA5-Land Reanalysis Database in Sicily, Italy. *Agric. Water Manag.* 2024, 295, 108732. [CrossRef]
- 78. Kraus, E.B. Subtropical Droughts and Cross-Equatorial Energy Transports. Mon. Weather Rev. 1977, 105, 1009–1018. [CrossRef]
- 79. Katz, R.W.; Glantz, M.H. Anatomy of a Rainfall Index. Mon. Weather Rev. 1986, 114, 764–771. [CrossRef]
- 80. Owens, R.; Hewson, T. ECMWF Forecast User Guide; ECMWF: Reading, UK, 2018. [CrossRef]
- 81. Hersbach, H. Decomposition of the Continuous Ranked Probability Score for Ensemble Prediction Systems. *Weather. Forecast.* **2000**, *15*, 559–570. [CrossRef]
- 82. Heinrich-Mertsching, C. SeaVal: Validation of Seasonal Weather Forecasts. R. Package Version 1 (2). 2024. Available online: https://CRAN.R-project.org/package=SeaVal (accessed on 1 March 2025).
- 83. Matheson, J.E.; Winkler, R.L. Scoring Rules for Continuous Probability Distributions. Manag. Sci. 1976, 22, 1087–1096. [CrossRef]
- 84. Gneiting, T.; Raftery, A.E. Strictly Proper Scoring Rules, Prediction, and Estimation. *J. Am. Stat. Assoc.* **2007**, *102*, 359–378. [CrossRef]
- 85. Normand, F.; Mathieu, L. Toward a Better Interpretation and Use of Thermal Time Models. *Acta Hortic.* **2006**, 707, 159–165. [CrossRef]
- 86. Steduto, P.; Hsiao, T.C.; Fereres, E.; Raes, D. *Crop Yield Response to Water*; FAO Irrig Drain Paper No. 66; FAO: Rome, Italy, 2012; 500p.
- 87. Jiménez-Jiménez, S.I.; de Jesús Marcial-Pablo, M.; Sánchez-Cohen, I.; Ojeda-Bustamante, W.; Inzunza-Ibarra, M.A.; Urrieta-Velazquez, J.A. Estimating Reference Evapotranspiration Using Reanalysis Data from the Google Earth Engine: A Case Study From an Arid Hydrological Region in Mexico. *Irrig. Drain.* 2025. [CrossRef]
- 88. Lopes, F.M.; Dutra, E.; Boussetta, S. Evaluation of Daily Temperature Extremes in the ECMWF Operational Weather Forecasts and ERA5 Reanalysis. *Atmosphere* **2024**, *15*, 93. [CrossRef]
- 89. Pelosi, A. Performance of the Copernicus European Regional Reanalysis (CERRA) Dataset as Proxy of Ground-Based Agrometeorological Data. *Agric. Water Manag.* **2023**, *289*, 108556. [CrossRef]
- 90. Gourgouletis, N.; Gkavrou, M.; Baltas, E. Comparison of Empirical ETo Relationships with ERA5-Land and In Situ Data in Greece. *Geographies* 2023, 3, 499–521. [CrossRef]
- 91. Weisheimer, A.; Palmer, T. On the Reliability of Seasonal Climate Forecasts. J. R. Soc. Interface R. Soc. 2014, 11, 20131162. [CrossRef]
- 92. Manzanas, R.; Torralba, V.; Lledó, L.; Bretonnière, P.A. On the Reliability of Global Seasonal Forecasts: Sensitivity to Ensemble Size, Hindcast Length and Region Definition. *Geophys. Res. Lett.* **2022**, *49*, e2021GL094662. [CrossRef]
- 93. Lundell, J.F.; Bean, B.; Symanzik, J. Let's Talk about the Weather: A Cluster-Based Approach to Weather Forecast Accuracy. *Comput. Stat.* **2023**, *38*, 1135–1155. [CrossRef]
- 94. Giunta, G.; Salerno, R.; Ceppi, A.; Ercolani, G.; Mancini, M. Benchmark Analysis of Forecasted Seasonal Temperature over Different Climatic Areas. *Geosci. Lett.* **2015**, 2, 9. [CrossRef]
- 95. Renan, L.R.; Katurji, M.; Zawar-Reza, P.; Quénol, H.; Sturman, A. Analysis of Spatio-temporal Bias of Weather Research and Forecasting Temperatures Based on Weather Pattern Classification. *Int. J. Climatol.* **2018**, *39*, 5784. [CrossRef]
- 96. Ji, F.; Evans, J.; Teng, J.; Scorgie, Y.; Argueso, D.; Di Luca, A. Evaluation of Long-Term Precipitation and Temperature Weather Research and Forecasting Simulations for Southeast Australia. *Clim. Res.* **2016**, *67*, 1366. [CrossRef]
- 97. Ferreira, G.W.S.; Reboita, M.S.; Drumond, A. Evaluation of ECMWF-SEAS5 Seasonal Temperature and Precipitation Predictions over South America. *Climate* **2022**, *10*, 128. [CrossRef]
- 98. Kioutsioukis, I.; de Meij, A.; Jakobs, H.; Katragkou, E.; Vinuesa, J.-F.; Kazantzidis, A. High Resolution WRF Ensemble Forecasting for Irrigation: Multi-Variable Evaluation. *Atmos. Res.* **2016**, *167*, 156–174. [CrossRef]
- 99. Patterson, M.; Befort, D.J.; O'Reilly, C.H.; Weisheimer, A. Drivers of the ECMWF SEAS5 Seasonal Forecast for the Hot and Dry European Summer of 2022. Q. J. R. Meteorol. Soc. 2024, 150, 4969–4986. [CrossRef]

100. Rolim, J.; Navarro, A.; Vilar, P.; Saraiva, C.; Catalao, J. Crop Data Retrieval Using Earth Observation Data to Support Agricultural Water Management. *Eng. Agrícola* **2019**, *39*, 380–390. [CrossRef]

- 101. French, A.N.; Sanchez, C.A.; Wirth, T.; Scott, A.; Shields, J.W.; Bautista, E.; Saber, M.N.; Wisniewski, E.; Gohardoust, M.R. Remote Sensing of Evapotranspiration for Irrigated Crops at Yuma, Arizona, USA. *Agric. Water Manag.* 2023, 290, 108582. [CrossRef]
- 102. Espírito Santo, F.; de Lima, M.I.P.; Ramos, A.M.; Trigo, R.M. Trends in Seasonal Surface Air Temperature in Mainland Portugal, since 1941. *Int. J. Climatol.* **2014**, *34*, 1814–1837. [CrossRef]
- 103. Cattiaux, J.; Ribes, A.; Cariou, E. How Extreme Were Daily Global Temperatures in 2023 and Early 2024? *Geophys. Res. Lett.* **2024**, 51, e2024GL110531. [CrossRef]
- 104. Copernicus Climate Change Service. The 2024 Annual Climate Summary—Global Climate Highlights 2024; 2025. Available online: https://climate.copernicus.eu/global-climate-highlights-2024 (accessed on 1 March 2025).
- 105. Soares, D.; Paço, T.A.; Rolim, J. Assessing Climate Change Impacts on Irrigation Water Requirements under Mediterranean Conditions—A Review of the Methodological Approaches Focusing on Maize Crop. *Agronomy* **2023**, *13*, 117. [CrossRef]

Disclaimer/Publisher's Note: The statements, opinions and data contained in all publications are solely those of the individual author(s) and contributor(s) and not of MDPI and/or the editor(s). MDPI and/or the editor(s) disclaim responsibility for any injury to people or property resulting from any ideas, methods, instructions or products referred to in the content.